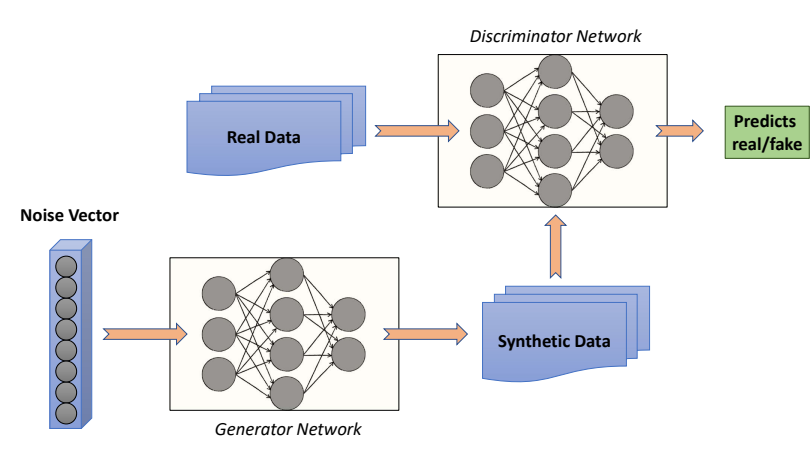




## GENERATIVE ADVERSARIAL NETWORKS (GANs)

- GANs [1] are generative models that learn to produce new samples from an unknown (real) distribution  $P_r$
- Generator  $G_\theta$  and discriminator  $D_\omega$  play an adversarial game
- $G_\theta$  maps noise  $Z$  to synthetic samples  $X_g$  to mimic the real samples  $X_r$ , while  $D_\omega$  tries to differentiate between the synthetic and real samples
- Formulated as a zero-sum min-max game:  $\inf_{G_\theta} \sup_{D_\omega} V(\theta, \omega)$



## VARIOUS VALUE FUNCTIONS & GANS

- Vanilla GAN (Goodfellow et al. [1]) minimizes Jensen-Shannon divergence (JSD):

$$\inf_{G_\theta} \sup_{D_\omega: \mathcal{X} \rightarrow [0,1]} \mathbb{E}_{X_r \sim P_r} [\log D_\omega(X_r)] + \mathbb{E}_{X_g \sim P_{G_\theta}} [\log(1 - D_\omega(X_g))] = 2\text{JSD}(P_r \| P_{G_\theta}) - \log 4$$

- Can reformulate GANs using class probability estimation (CPE) loss  $\ell(y, \hat{y})$ ,  $(y, \hat{y}) \in \{0, 1\} \times [0, 1]$  [2, 3] as

$$\inf_{G_\theta} \sup_{D_\omega: \mathcal{X} \rightarrow [0,1]} (V_\ell(\theta, \omega) := \mathbb{E}_{X_r \sim P_r} [-\ell(1, D_\omega(X_r))] + \mathbb{E}_{X_g \sim P_{G_\theta}} [-\ell(0, D_\omega(X_g))])$$

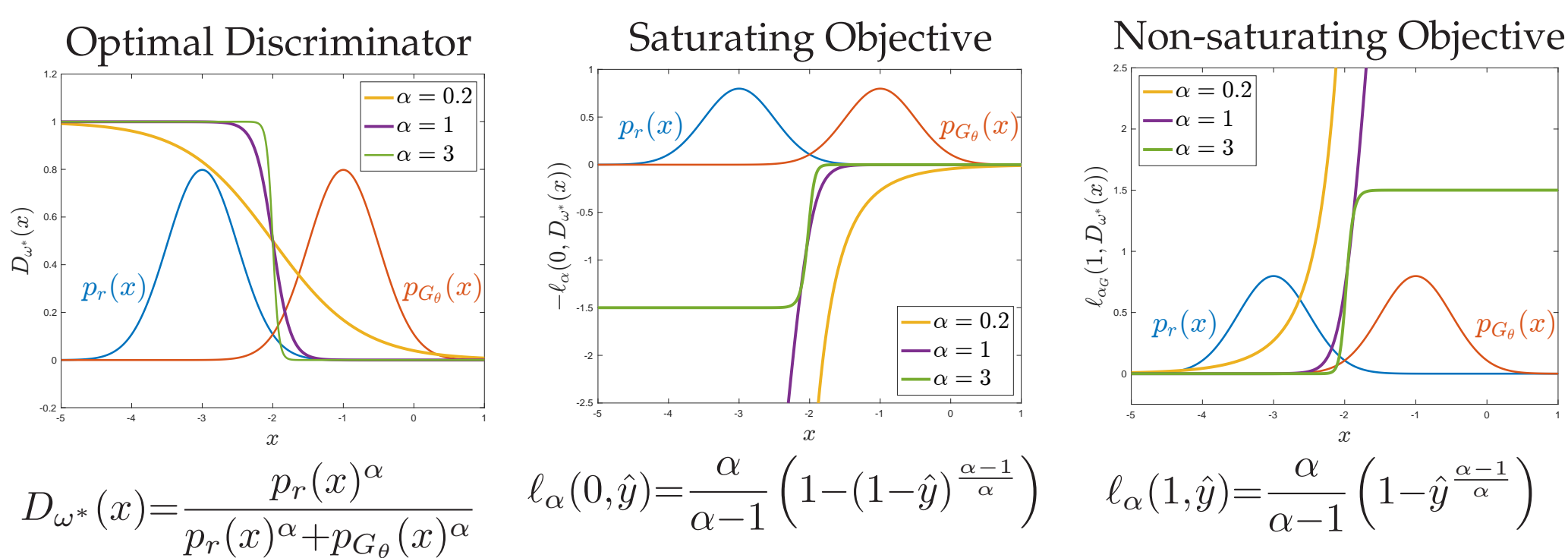
- We obtain  $\alpha$ -GAN using  $\alpha$ -loss (Sypherd et al. [4])

$$\ell_\alpha(y, \hat{y}) = \frac{\alpha}{\alpha - 1} \left( 1 - y\hat{y}^{\frac{\alpha-1}{\alpha}} - (1-y)(1-\hat{y})^{\frac{\alpha-1}{\alpha}} \right), \text{ for } \alpha \in (0, 1) \cup (1, \infty)$$

- $\alpha$ -GAN minimizes the Arimoto divergence and recovers vanilla GAN ( $\alpha \rightarrow 1$ ), Hellinger GAN ( $\alpha = 1/2$ ), and total variation (TV) GAN ( $\alpha \rightarrow \infty$ )

## TRAINING INSTABILITIES IN GANS

Toy example:  $P_r = \mathcal{N}(-3, 0.5)$ ,  $P_{G_\theta} = \mathcal{N}(-1, 0.5)$



- Vanilla GAN generator's objective can saturate when discriminator confidently classifies generated data as fake; tuning  $\alpha < 1$  addresses *vanishing gradients* by reducing confidence of discriminator
- However,  $\alpha \leq 1$  can produce *exploding gradients* for the generator as the generated samples approach real samples, potentially resulting in the generated data being repelled from the real data
- [1] proposed a *non-saturating* alternative generator objective to combat vanishing gradients:

$$\mathbb{E}_{X_g \sim P_{G_\theta}} [-\log(1 - D_\omega(X_g))]$$

- However, this objective can still lead to *model oscillation* and even *mode collapse* due to failure to converge and sensitivity to hyperparameter initialization (e.g. learning rate) because of large gradients

- Can address all of these types of instabilities via different  $\alpha$  values for discriminator and generator losses

## $(\alpha_D, \alpha_G)$ -GANs: DUAL OBJECTIVES

- Saturating  $(\alpha_D, \alpha_G)$ -GAN [5] non-zero sum game given by:

$$\sup_{D_\omega: \mathcal{X} \rightarrow [0,1]} V_{\ell_{\alpha_D}}(\theta, \omega) \quad \inf_{G_\omega} V_{\ell_{\alpha_G}}(\theta, \omega)$$

**Result.** For a fixed  $G_\omega$ , the  $D_\omega^*$  of an  $(\alpha_D, \alpha_G)$ -GAN is the same as that of  $\alpha$ -GAN with  $\alpha = \alpha_D$ . For this  $D_\omega^*$  and for  $(\alpha_D, \alpha_G) \in (0, \infty]^2$  such that  $(\alpha_D \leq 1, \alpha_G > \alpha_D/(\alpha_D + 1))$  or  $(\alpha_D > 1, \alpha_D/2 < \alpha_G \leq \alpha_D)$ , the generator of a saturating  $(\alpha_D, \alpha_G)$ -GAN minimizes a non-negative symmetric  $f$ -divergence.

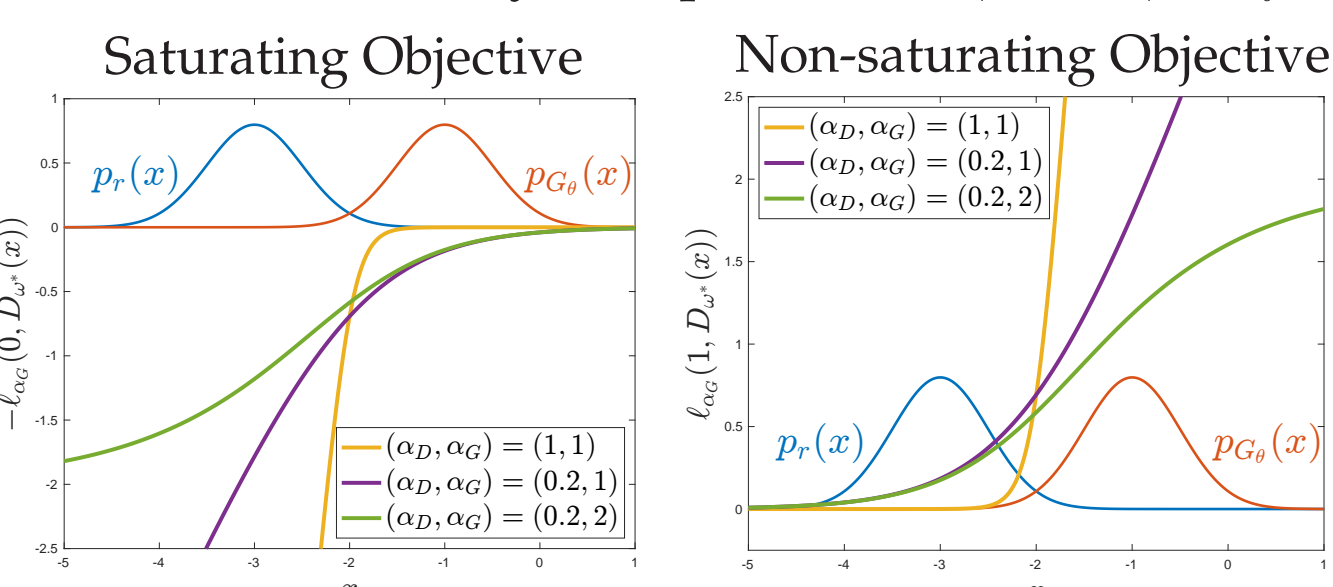
- Non-saturating  $(\alpha_D, \alpha_G)$ -GAN given by:

$$\sup_{D_\omega: \mathcal{X} \rightarrow [0,1]} V_{\ell_{\alpha_D}}(\theta, \omega) \quad \inf_{G_\omega} \mathbb{E}_{X_g \sim P_{G_\theta}} [\ell_{\alpha_G}(1, D_\omega(X_g))]$$

**Result.** For the same  $D_\omega^*$  and for  $(\alpha_D, \alpha_G) \in (0, \infty]^2$  with  $\alpha_D + \alpha_G > \alpha_G \alpha_D$ , the generator of a non-saturating  $(\alpha_D, \alpha_G)$ -GAN minimizes a non-negative asymmetric  $f$ -divergence.

## $(\alpha_D, \alpha_G)$ -GANs: TOY EXAMPLE

Toy example:  $P_r = \mathcal{N}(-3, 0.5)$ ,  $P_{G_\theta} = \mathcal{N}(-1, 0.5)$



Tuning  $\alpha_D < 1$  and  $\alpha_G = 1$  produces more gradient for the generator while making its objective less convex, which helps stabilize training; tuning  $\alpha_G > 1$  results in a quasiconvex generator objective, which can further improve training stability

## ILLUSTRATION OF RESULTS

- **2D-ring dataset:** samples drawn from a mixture of 8 equal-prior Gaussian distributions (modes), indexed  $i \in \{1, 2, \dots, 8\}$  with mean  $(\cos(2\pi i/8), \sin(2\pi i/8))$  and variance  $10^{-4}$

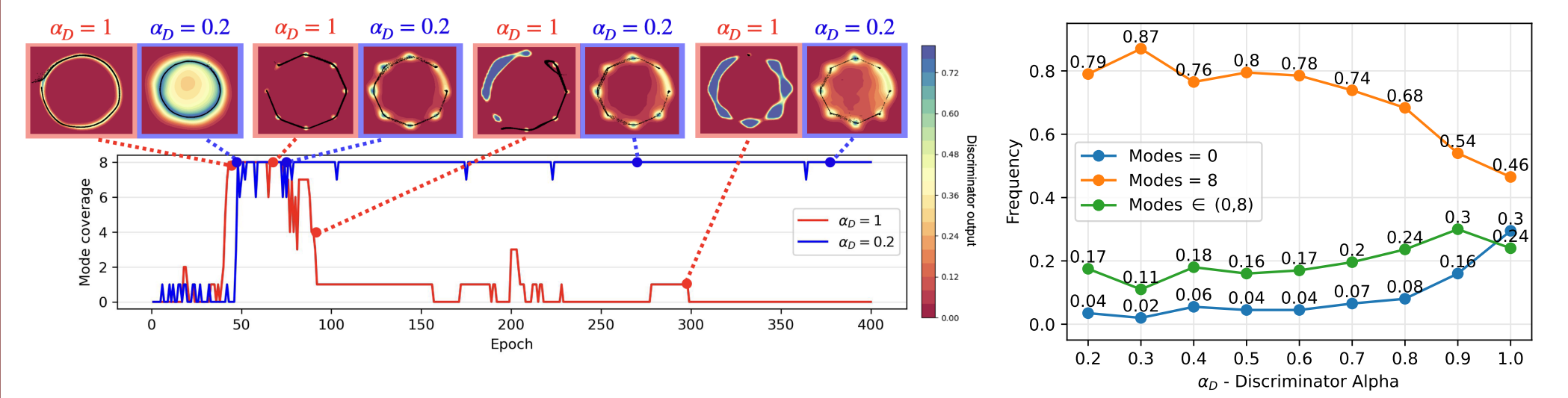


**Figure 1:** (Left) Plot of mode coverage over epochs for saturating  $(\alpha_D, \alpha_G)$ -GAN, fixing  $\alpha_G = 1$ . (Right) Plot of success and failure rates over 200 seeds for a range of  $\alpha_D$  values with  $\alpha_G = 1$ .

- **Celeb-A dataset:** collection of over 200,000 celebrity headshots, resized to  $64 \times 64$
- Compare performance of non-saturating vanilla GAN, non-saturating  $(\alpha_D, \alpha_G)$ -GANs and Least Squares GAN (LSGAN) [6] with 0-1 binary coding scheme ( $a = 0, b = c = 1$ ):

$$D: \inf_{\omega \in \Omega} \mathbb{E}_{X_r \sim P_r} \left[ \frac{1}{2} (D_\omega(X_r) - b)^2 \right] + \mathbb{E}_{X_g \sim P_{G_\theta}} \left[ \frac{1}{2} (D_\omega(X_g) - a)^2 \right]$$

$$G: \inf_{\theta \in \Theta} \mathbb{E}_{X_g \sim P_{G_\theta}} \left[ \frac{1}{2} (D_\omega(X_g) - c)^2 \right]$$

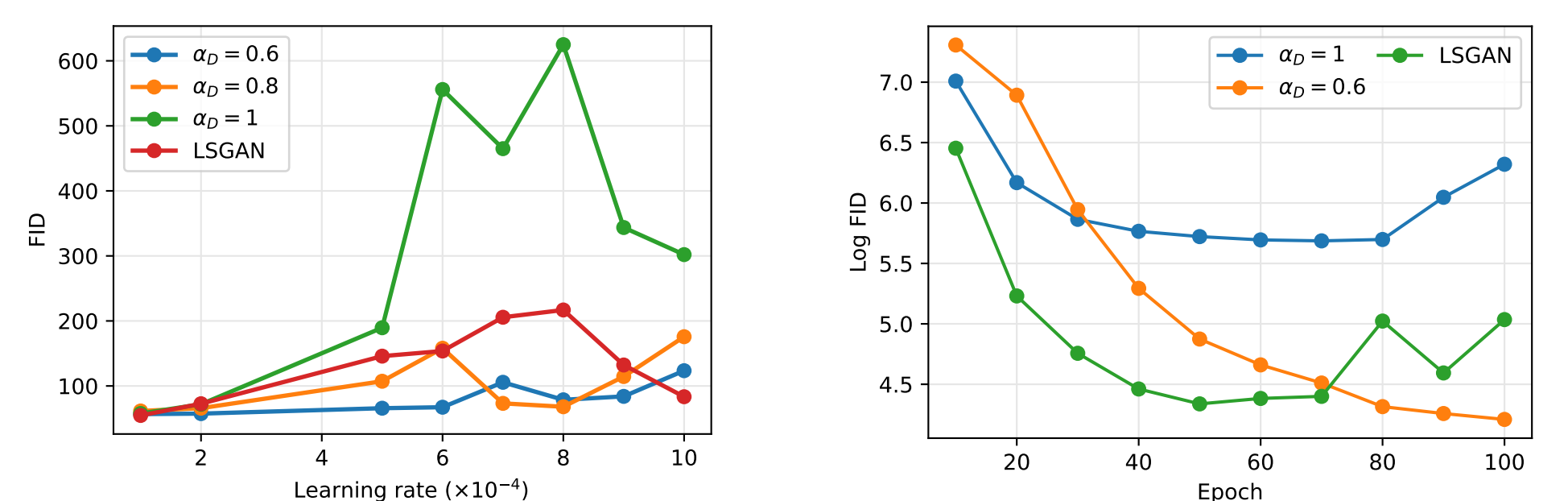


**Figure 2:** (Left) Plot of FID (smaller is better) averaged over 50 seeds vs. learning rate for a fixed number of epochs ( $=100$ ) and different non-saturating  $(\alpha_D, \alpha_G = 1)$ -GANs as well as LSGAN. (Right) Log-scale plot of FID over training epochs for the non-saturating  $(1, 1)$ -GAN (vanilla), the non-saturating  $(0.6, 1)$ -GAN and LSGAN with learning rate  $6 \times 10^{-4}$ .

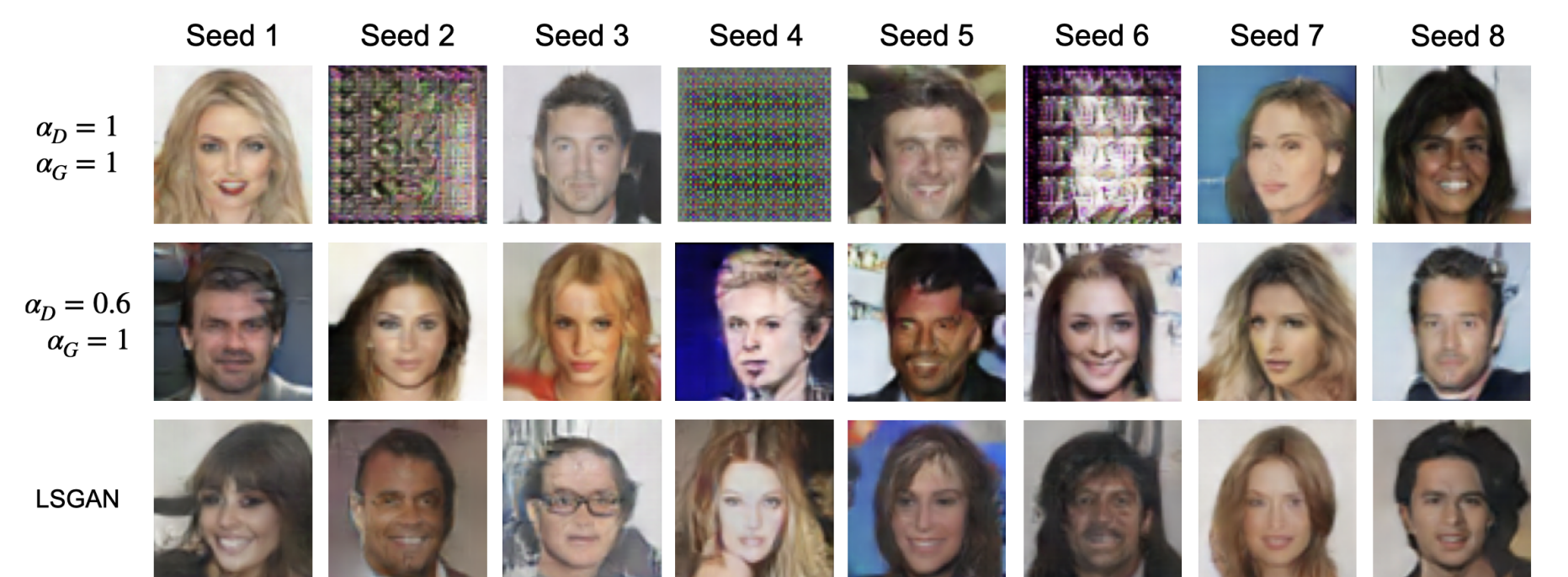


**Figure 3:** Generated Celeb-A faces from the non-saturating  $(1, 1)$ -GAN (vanilla), the non-saturating  $(0.6, 1)$ -GAN and LSGAN over 8 seeds when trained for 100 epochs with a learning rate of  $5 \times 10^{-4}$ .

- **LSUN Classroom dataset:** contains over 150,000 classroom images, resized to  $112 \times 112$

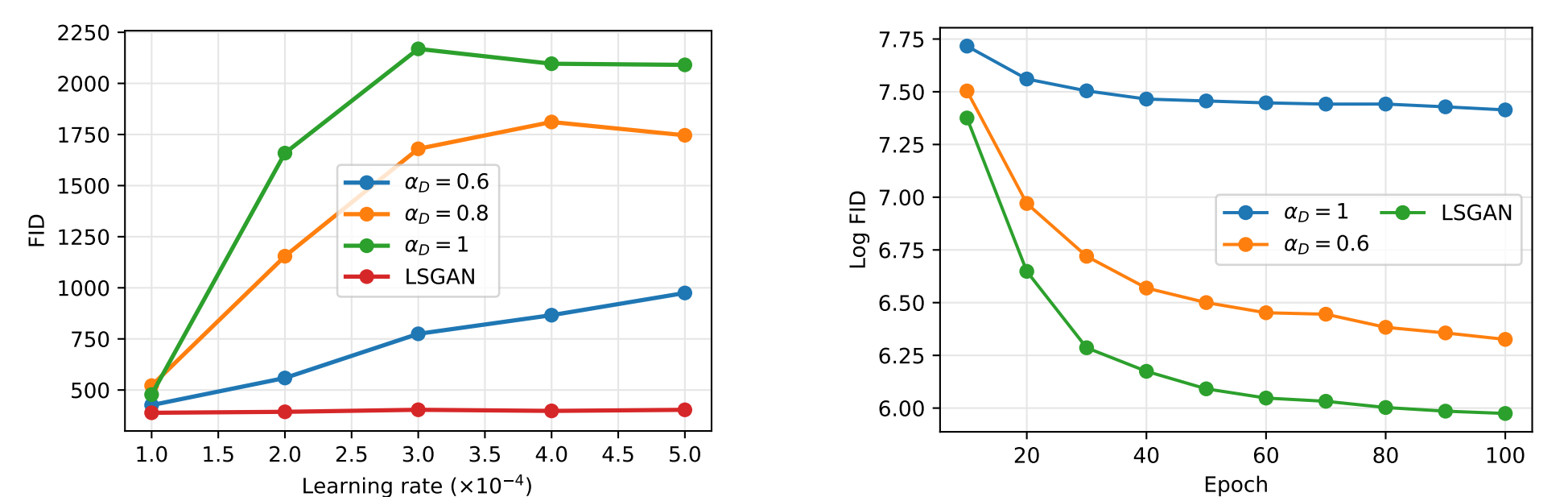


**Figure 4:** (Left) Plot of FID (smaller is better) averaged over 50 seeds vs. learning rate for a fixed number of epochs ( $=100$ ) and different non-saturating  $(\alpha_D, \alpha_G = 1)$ -GANs as well as LSGAN. (Right) Log-scale plot of FID over training epochs for the non-saturating  $(1, 1)$ -GAN (vanilla), the non-saturating  $(0.6, 1)$ -GAN and LSGAN with learning rate  $2 \times 10^{-4}$ .

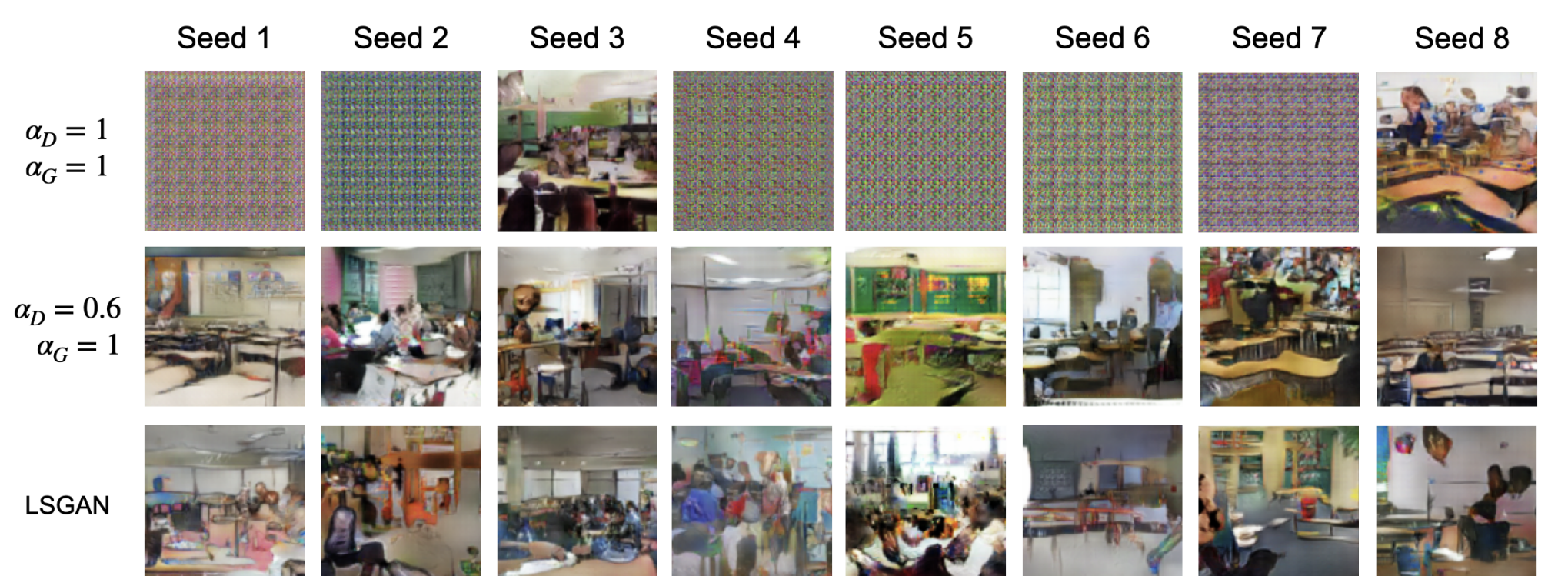


**Figure 5:** Generated LSUN Classroom images from the non-saturating  $(1, 1)$ -GAN (vanilla), the non-saturating  $(0.6, 1)$ -GAN and LSGAN over 8 seeds when trained for 100 epochs with a learning rate of  $2 \times 10^{-4}$ .

**Takeaway:**  $\alpha_D < 1, \alpha_G \geq 1$  more robust to hyperparameter initialization, helping to alleviate training instabilities; restricted  $\alpha_D, \alpha_G$  ranges make this computationally feasible

## ACKNOWLEDGMENTS & REFERENCES

- Work supported by NSF grants CIF-1901243, CIF-1815361, CIF-2007688, CIF-2134256, SaTC-2031799, SCH-2205080
- [1] Goodfellow et al. Generative adversarial nets. In *NeurIPS*, 2014.
  - [2] Kurri et al. Realizing GANs via a tunable loss function. In *ITW*, 2021.
  - [3] Kurri et al.  $\alpha$ -GAN: Convergence and estimation guarantees. In *ISIT*, 2022.
  - [4] Sypherd et al. A tunable loss function for robust classification: Calibration, landscape, and generalization. *IEEE Trans. on Inf. Theory*, 2022.
  - [5] Welfert et al.  $(\alpha_D, \alpha_G)$ -GANs: Addressing GAN training instabilities via dual objectives. In *ISIT*, 2023.
  - [6] Mao et al. Least squares generative adversarial networks. In *ICCV*, 2017.